

Photometric Standards for Raman Spectroscopy

Richard L. McCreery

Reproduced from:

Handbook of Vibrational Spectroscopy

John M. Chalmers and Peter R. Griffiths (Editors)

© John Wiley & Sons Ltd, Chichester, 2002

Photometric Standards for Raman Spectroscopy

Richard L. McCreery

Ohio State University, Columbus, OH, USA

1 INTRODUCTION

Although Raman scattering has been studied for just over 70 years, recent technological advances have greatly broadened its applicability to materials characterization and chemical analysis.^{1–5} Low noise multichannel detectors, efficient spectrographs, and fiber optic techniques have boosted Raman signal strength by as much as a factor of 10^5 , while Fourier transform (FT)-Raman and near-infrared (NIR) excitation have greatly reduced interferences from fluorescence. These advances comprise a revolution in Raman instrumentation which has led to new applications in process monitoring, pharmaceutical analysis, microscopy, and surface analysis, among many others. It appears that Raman spectroscopy has the prospect to become as routine as Fourier transform infrared (FT-IR), with the special advantages of noninvasive sampling, compatibility with water and common optical materials, and provision for remote sampling.

Both historically and currently, the majority of applications of Raman spectroscopy are qualitative, with the objectives often being determination of peak frequencies and comparison of vibrational features to spectra from different laboratories, or predicted theoretically. The great majority of reported Raman spectra are not corrected for variation of instrumental sensitivity across the spectrum, and the intensity scale is often arbitrary. Unlike UV–vis (ultraviolet–visible) and infrared (IR) absorption spectroscopy, Raman scattering is observed in a “single beam” mode, without a reference channel to compensate for instrumental sensitivity variation with time or wavelength.^{5,6} As a result, it is generally difficult to compare relative or absolute Raman intensities from different instruments,

and calibration transfer based on intensities is exceedingly difficult. The problem is compounded by the dependence of observed Raman intensity on focusing and alignment, so that a given sample may yield significant variation of intensity from day to day, even on a particular instrument and under apparently identical conditions. Although Raman has been a very valuable probe of molecular structure and orientation, the difficulty in reliable determination of relative and absolute intensities has impeded its utility as a quantitative technique. There are certainly examples of quantitative Raman spectroscopy, but they usually involve a daily calibration which applies only to a particular spectrometer.

As discussed in more detail in Section 3, there are several motivations for increasing the reproducibility and accuracy of a Raman intensity scale. At the least, a calibration of the intensity scale permits observation of changes in a particular instrument over time, or between several similar instruments. If sensitivity or reproducibility is a criterion for experimental design, different instruments and configurations may be compared for a given photometric standard. Library searching can be based both on peak positions and relative peak intensities, and will be more effective when the intensity scales of the sample spectrum and library spectrum are the same. Furthermore, if the user wants to subtract a library spectrum from an “unknown” spectrum to search for additional components, the subtraction is much more effective when both spectra use the same intensity scale. This is illustrated in Figure 1, which compares an uncorrected spectrum of a commercial pharmaceutical tablet with a corrected spectrum of the active ingredient from a library. The spectrometer response varied across the spectrum, causing distortion of relative intensities and resulting in a residue after subtraction of the library spectrum of the active ingredient. In addition, calibrated Raman intensity permits evaluation of the relative strengths of various materials as

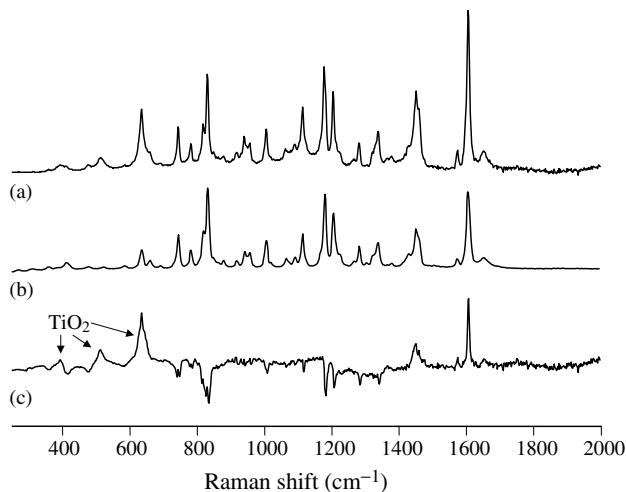


Figure 1. Raman spectra (785 nm laser) for (a) “Motrin” pain reliever (uncorrected for instrumental response) and (b) ibuprofen (corrected) in a spectral library; (c) is the difference spectrum. Note, ibuprofen features cannot be accurately subtracted due to distortion of relative intensities in the uncorrected spectrum. (Adapted from Reference 5, with permission.)

Raman scatterers. More precisely, comparisons of scattering intensities permit assessment of Raman cross-sections, thus permitting evaluations of the feasibility of Raman detection. Finally, a Raman spectrum should reflect the actual Raman scattering efficiency of vibrational features in a given molecule, unperturbed by variations of instrumental design or experimental procedure. Before Raman spectroscopy can be established as a reliable technique subject to successful regulatory scrutiny, standard procedures and materials for calibrating Raman intensity must be developed and approved.

2 THEORY

There exists a wide variety of expressions for Raman intensity as a function of experimental variables, which apply to different situations and different experimental configurations. None of these could be considered to be a convention at present, but it is worth describing some signal expressions to provide a context for the remainder of the article. A convenient approach is to separate the sample and laser variables from the collection and detection variables by means of the definition of specific intensity. Equation (1) expresses specific intensity, L , in terms of the laser power density P_D (in photons $\text{s}^{-1} \text{cm}^{-2}$), the differential Raman cross-section, β (in $\text{cm}^2 \text{molecule}^{-1} \text{sr}^{-1}$) and number density of scatterers D (in molecules cm^{-3}). Although Raman spectroscopists rarely state concentration in terms of molarity, equation (1) may be stated with D in moles per liter by multiplying β by 6.02×10^{20} to yield

units of $\text{molar}^{-1} \text{cm}^{-1} \text{sr}^{-1}$.

$$L \text{ (photons } \text{sr}^{-1} \text{cm}^{-2} \text{s}^{-1}) = P_D \beta D K \quad (1)$$

The path length K (in cm) depends on sampling geometry, but in many situations equals the sample path length monitored by the spectrometer. The cross-section, β , is commonly listed as $d\sigma/d\Omega$, and in this article will be referred to as the differential Raman cross-section. β depends both upon observation geometry and laser frequency, and is often determined empirically for a given application and spectrometer. (β is “differential” with respect to observation angle ($d\Omega$) but it is integrated over the entire frequency range of the Raman band of interest.) The frequency dependence of both the differential and integrated Raman cross-section have been studied extensively and a few compilations of cross-sections are available.^{7–9} The frequency dependence of β is given by equation (2), where β_j^o is defined as a frequency-independent cross-section of the j th vibrational mode.

$$\beta_j = \beta_j^o \tilde{\nu}_0 (\tilde{\nu}_0 - \tilde{\nu}_j)^3 \quad (2)$$

where $\tilde{\nu}_0$ is the wavenumber of the laser and $\tilde{\nu}_j$ is the wavenumber of the j th vibrational transition.

An important issue arises at this point, because the frequency dependence of the cross-section can depend on the way the Raman measurement is performed. Equation (2) applies to the case where the signal is obtained by counting photons over a pixel or frequency increment, as is the case with most dispersive/charge-coupled device (CCD) spectrometers. If scattered power is measured rather than the number of scattered photons, equation (3) applies.

$$\beta'_j = \beta_j^o (\tilde{\nu}_0 - \tilde{\nu}_j)^4 \quad (3)$$

Classical Raman spectrometers as well as many modern FT Raman spectrometers measure power rather than photons and the frequency dependence of equation (3) applies. A further consequence of this experimental factor is a change in relative intensities when a Raman spectrum is plotted as power vs wavelength rather than photons or photons/second vs wavelength. Since the energy per photon changes across the observed Raman shift range, the two representations differ by a factor of $\tilde{\nu}_0/(\tilde{\nu}_0 - \tilde{\nu}_j)$. This difference is relatively small for visible and UV Raman spectrometers since the wavelength interval is fairly small for the usual range of Raman shifts. However, in the NIR region at wavelengths above about 700 nm, the normal Raman shift range covers a significant range of wavelength, and the difference in representation can yield quite different relative peak intensities. For example, with a 1064 nm laser, the relative intensities of the CH stretch and 801 cm^{-1}

bands of cyclohexane differ by 32% when measured in watts as opposed to photons per second.

Equations (2) and (3) apply in the absence of resonance or preresonant enhancement. When the laser frequency is near an electronic absorption of the sample molecule there can be significant departures from the frequency dependence expected from equation (2) or (3). The effect of resonance on the observed cross-sections is highly variable and dependent on the sample. Equation (4) was presented by Albrecht and Huntley,¹⁰ and has been verified experimentally for several cases.¹¹⁻¹⁵

$$\beta = k\tilde{\nu}_0(\tilde{\nu}_0 - \tilde{\nu}_j)^3 \left[\frac{\tilde{\nu}_p^2 + \tilde{\nu}_0^2}{(\tilde{\nu}_p^2 - \tilde{\nu}_0^2)^2} \right]^2 \quad (4)$$

When the laser frequency ($\tilde{\nu}_0$) differs significantly from an electronic absorption of the molecule ($\tilde{\nu}_p$), the ratio in equation (4) changes slowly with laser frequency, and the frequency dependence of β reverts to that of equation (2). However, as the laser frequency approaches an electronic absorption, the cross-section increases greatly. A further complication when resonance effects are present is the absorption of both laser light and Raman scattered light by the sample.¹⁶ The result is nonconstant power density in equation (1), and a complex dependence of Raman intensity on both concentration and sample depth. In these cases it is possible to calibrate the spectrometer response, but sample variables will affect both relative and absolute peak intensities.

Once an equation relating the specific intensity to laser to sample variables is in hand, we can turn to the collection and detection of scattered light. A collection function may be defined which states the fraction of total scattered light that is collected, analyzed, and detected by the spectrometer. Equations (5) and (6) state the observed signal in terms of a collection function, C , and equations (7) and (8) state the signal as a function of a variety of experimental variables.¹⁷

$$S(e^-) = LCt \quad (5)$$

$$C(\text{cm sr e photon}^{-1}) = A_D \Omega_D T Q \quad (6)$$

$$S(e^-) = LA_D \Omega_D T Q t \quad (7)$$

$$S(e^-) = (P_D \beta DK)(A_D \Omega_D T Q)t \quad (8)$$

where $S(e^-)$ is the observed signal (in photoelectrons), t is the observation time (in seconds), A_D is the sample area monitored by the spectrometer (in cm^2), Ω_D is the collection solid angle of the spectrometer, at the sample (in sr), T is the transmission of the spectrometer and collection optics (unitless), and Q is the quantum efficiency of the detector, (in e- per photon).

When considering photometric accuracy in Raman spectroscopy the most basic issue is the relationship between the observed signal and sample variables such as cross-section and concentration. Unfortunately, this basic objective is difficult to achieve because it depends on the large number of variables in equation (8). This issue may be appreciated by a pragmatic comparison of absorption techniques to Raman scattering. In absorption spectroscopy such as FT-IR, there is a reference spectrum which effectively calibrates most instrumental variables. Although detector response, source intensity, and optical losses are relevant to an absorption experiment, their effects are removed from the final spectrum by calculating a ratio of reference and sample spectra. In Raman spectroscopy, however, one usually measures only the scattered intensity with no reference beam. So variations in the collection function with time or with wavelength are not compensated by a reference spectrum. The difference between a double beam absorption measurement and a single beam Raman experiment serves to define the objectives of this article.

3 OBJECTIVES

The article describes three steps toward achievement of a corrected Raman spectrum which accurately represents the scattering intensity of a given sample as a function of Raman shift:

1. Reproducibility of observed scattering intensity.
2. Correction for variation of instrument response across a Raman spectrum.
3. Determination of absolute scattering intensity and absolute Raman cross-sections.

As discussed below, the first two objectives may be achieved by straightforward calibration, while the third is much more involved. Fortunately, the great majority of Raman applications do not require assessment of absolute intensity, with the accompanying experimental difficulties. Reproducible Raman intensities may be achieved with sensible design of sampling optics and reasonable experimental care. Although response function correction is not yet routine, it is readily applied and quite useful. The result of these two calibration steps is a Raman spectrum which accurately reflects relative Raman scattering intensities and is useful for library searching, quantitative analysis, and comparison of spectra between laboratories. Current applications of Raman spectroscopy can be broadened significantly without calibrating absolute intensity, and absolute measurements of cross-sections are generally left to the specialist.

4 REPRODUCIBILITY OF INTENSITY

The most basic issue regarding photometric accuracy in Raman spectroscopy is reproducibility of observed intensity. Since Raman intensity depends upon the variables contained in equation (8) as well as focus, alignment, etc., intensity reproducibility is not a trivial matter. Furthermore, properties of the sample such as optical transparency and homogeneity can affect observed intensity, even when the overall sample composition is fixed. Some factors which affect observed intensity are discussed in the following.

4.1 Shot noise

A Raman measurement is based ultimately on counting photons, and is governed by Poisson statistics. Even for repetitive measurements of a rigidly mounted sample and perfectly constant laser power, the standard deviation of the signal equals $S^{1/2}$, where S is the observed signal in electrons. Restated, the relative standard deviation (RSD) of repetitive runs is at least $S^{-1/2}$ at the shot noise limit. For example, a signal with an average magnitude of 10000 electrons has a minimum RSD of 1%.

4.2 Sample alignment and focus

The overlay of sample, laser focus, and sampled volume of the collection optics determines the product $A_D K$ in equation (8), as shown for the case of 180° backscattering geometry in Figure 2. The sampled volume equals the volume defined by the laser beam cross-section along the sample length observed by the spectrometer. The sample length in Figure 3 is either the sample thickness or the depth

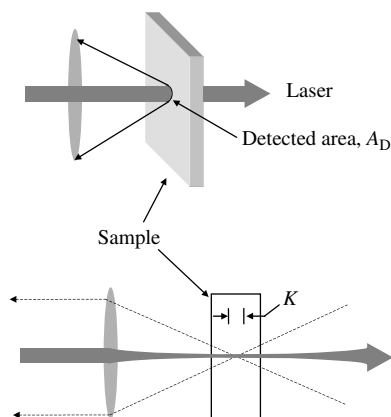


Figure 2. Superposition of sample, laser focus, and collection optics for 180° backscattering geometry. K in equations (1) and (8) is determined by the length of overlap between the sample and the collection depth of field.

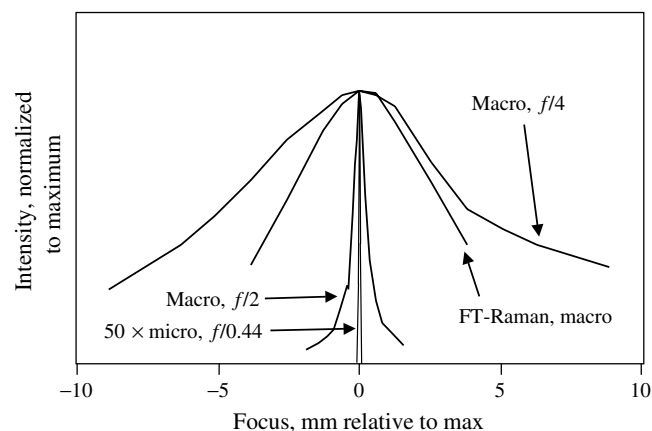


Figure 3. Intensity of silicon 521 cm^{-1} band for four spectrometers with varying depth of focus, normalized to the intensity at optimum focus. “Micro” refers to sampling through a microscope objective, while “macro” refers to conventional lenses. All cases used 180° backscattering geometry. (Adapted from Reference 5, with permission.)

of field of the spectrometer, whichever is smaller. A rigorous determination of the product $P_D A_D K$ in equation (8) requires integration of the product of the laser power density and sample number density over the sampled volume. This rigorous approach is quite impractical, so variations in power density across the beam diameter and along the sample length are usually ignored (as in equation 8), and the effective sampled volume is determined empirically with a known sample. Misalignment of laser and collection optics will decrease the effective sampling volume, with obvious consequences to the signal. Such misalignments are usually avoided by rigid mounts for the sample, laser optics and collection optics.

4.3 Spectrometer depth of focus

Raman spectrometers differ significantly in their sampling depth for transparent samples, from a few micrometers for a Raman microscope to several millimeters for conventional sampling. Depth of focus obviously affects signal magnitude, but also affects the degree to which the signal is sensitive to positioning. A short depth of focus requires more precise positioning, so the RSD for repetitive sampling will usually be larger. Figure 3 shows the variation of signal with focusing for several spectrometers whose depths of focus range from $<2\ \mu\text{m}$ to $>2\ \text{mm}$. Focusing reproducibility is particularly critical for Raman microscopes, since they usually operate with low $f/\#$ and short depth of focus.¹⁸

4.4 Sample absorption and scattering

An absorbing sample attenuates both the incident laser light and the Raman shifted photons leaving the sample. Powders

or polycrystalline materials also exhibit elastic scattering of incident and Raman light, thus affecting the size of the sampled volume. Absorption and scattering usually follow an exponential dependence, with an attenuation constant which combines absorption and scattering, as in equation (9) for the case of backscattering geometry.

$$P_D(z) = P_D(z = 0) e^{-\alpha_L z} \quad (9)$$

where $P_D(z)$ is the laser power density at sample depth z , $P_D(z = 0)$ is the incident laser power density, α_L is the combined absorption and scattering coefficient at laser wavelength, and z is the depth into the sample from the surface.

The Raman scattered light is governed by a similar equation and a coefficient at the Raman scattered wavelength (α_R), leading to an expression for K in an absorbing sample:¹⁹

$$K = \int_0^b e^{-(\alpha_L + \alpha_R)z} dz = \frac{1 - e^{-(\alpha_L + \alpha_R)b}}{\alpha_L + \alpha_R} \quad (10)$$

Finally, if the sample is optically dense, so that the laser light is completely absorbed or attenuated within the sample, $b \gg (\alpha_L + \alpha_R)^{-1}$, and:

$$S = \frac{P_D \beta D A_D \Omega_D T t}{\alpha_L + \alpha_R} \quad (11)$$

4.5 Sample heterogeneity

Most Raman spectrometers use a fairly small laser focus (1–100 μm diameter, typically), and sample a small region of a given sample. If the sample is heterogeneous on a size scale comparable to the laser focus, there may be significant variation in Raman intensity, depending upon which sample component is observed. For example, pharmaceutical tablets often are pressed from physical mixtures of several powders with particles in the range of 10–50 μm . A 25 μm laser focus will generate a Raman spectrum which is heavily biased by the composition of the particle at the focus, and repetitive sampling of a given tablet may yield large spectroscopic signal variations. If the laser spot is larger (or particle size is smaller), the Raman spectrum represents a spatial average over the laser spot area, which approaches the bulk composition as the spot size increases.

Table 1 lists several observed standard deviations of Raman peak intensities for several sampling situations. For repetitive acquisition from a motionless sample (lines 1 and 2), the RSD is determined by shot noise. For a signal of 25 000 electrons (the approximate signal for line 1), the predicted RSD from shot noise alone is 0.63%, and decreases to 0.28% for a longer integration time (line

Table 1. Reproducibility of Raman signal for 180° geometry.^{a,b}

Sample	Integration time ^c (s)	Relative standard deviation ^d (%)
1. CH ₂ Cl ₂ in cuvette, motionless	0.5	0.63
2. CH ₂ Cl ₂ in cuvette, motionless	2.5	0.31
3. CH ₂ Cl ₂ , remove and replace	2.5	0.82
4. Clear, solid polystyrene	2.5	0.78
5. Silicon wafer, remove and replace.	10	0.78
6. Heterogeneous tablet, ^e motionless	1.5	0.70
7. Tablet, ^e remove and replace	1.5	13
8. Tablet, defocused, remove and replace	1.5	3.1
9. Tablet, line focus, spinning, remove and replace sample	1.5	1.5

^aChromex Raman 2000, backscattering geometry, focal length = 75 nm, $f/4$.

^bAdapted from McCreery.⁵

^cFor each run of a set of 10.

^dObserved, for peak heights of 10 spectra.

^eAcetaminophen, cellulose, magnesium stearate pressed tablet, heterogeneous on a roughly 50 μm scale.

2). The agreement with the experimental results implies that the measurement is truly limited by shot noise, and a lower RSD may be obtained only by longer integration time. Lines 3, 4 and 5 list the RSD observed for methylene chloride, polystyrene, and silicon which were removed and replaced (without refocusing) between each of 10 runs. The RSD is larger (0.78–0.82%) due to small errors in sample repositioning. Lines 6–9 illustrate the effect of sample heterogeneity for the case of a pressed tablet containing three components (acetaminophen, magnesium stearate, microcrystalline cellulose) had a large RSD for a laser point focus (13%), which decreased to 6% for a line focus, and to 1.5% for a line focus and a spinning sample (~ 5 revolutions per second). As the area monitored by the laser increased, the spectrometer effectively spatially averaged over a larger area and the spectrum more accurately reflected the bulk composition of the sample.

5 RESPONSE FUNCTION CALIBRATION

An example of the consequences of variations of instrument response function is shown in Figure 4. The true spectra of cyclohexane obtained with 785 and 514.5 nm lasers differ only slightly in relative band intensities, due to the variations in cross-section with laser frequency embodied in equations (2) and (3). For the example of cyclohexane, the peak area of any band j relative to the area of the 801 cm^{-1}

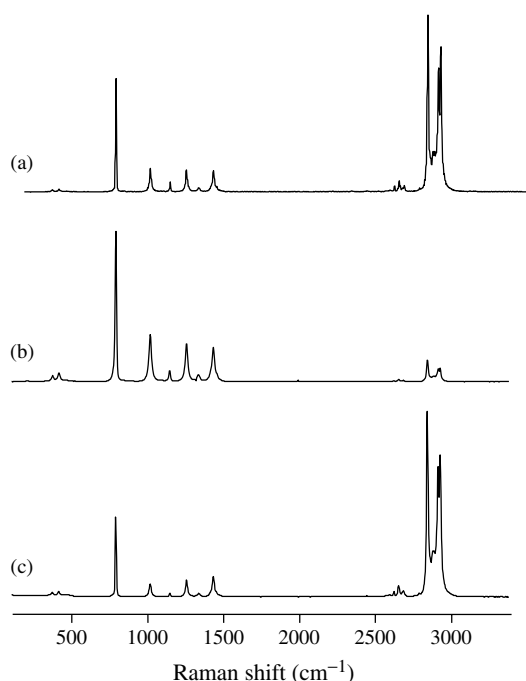


Figure 4. Uncorrected Raman spectra of cyclohexane obtained with three spectrometers, operating at (a) 514.5 nm, (b) 785 nm, and (c) 1064 nm.

band is given by equation (12).

$$\frac{A_j}{A_{801}} = \frac{\beta_j}{\beta_{801}} = \frac{\beta_j^0 (\tilde{\nu}_0 - \tilde{\nu}_j)^3}{\beta_{801}^0 (\tilde{\nu}_0 - 801)^3} \quad (12)$$

If A_j/A_{801} is the peak area ratio for a different laser frequency, it may be calculated from equation (13), which follows from equation (12) expressed for two laser frequencies:

$$\frac{A'_j}{A'_{801}} = \left[\frac{A_j (\tilde{\nu}'_0 - \tilde{\nu}_j)^3 (\tilde{\nu}_0 - 801)^3}{A_{801} (\tilde{\nu}'_0 - 801)^3 (\tilde{\nu}_0 - \tilde{\nu}_j)^3} \right] \quad (13)$$

For example, equation (13) predicts that the A_{1444}/A_{801} ratio decreases by 6% when the laser is changed from 515 to 785 nm, and the A_{CH}/A_{801} ratio decreases by 20%. Table 2 lists predicted relative peak areas of cyclohexane for several

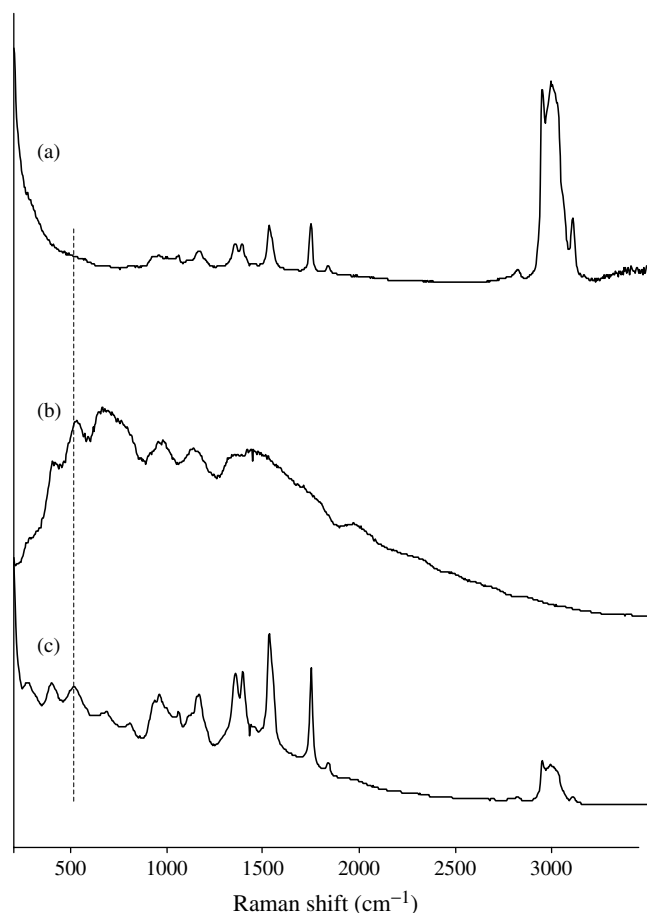


Figure 5. Corrected spectrum (a) of canola oil obtained at 785 nm on a dispersive/CCD spectrometer (Chromex 2000). (b) Spectrometer response function; (c) uncorrected spectrum. The dotted line indicates the location of a modulation in the response function caused by the laser rejection filter.

laser wavelengths, calculated using equation (13). The final column lists relative peak areas expected for FT-Raman when power is monitored rather than photons per second.

The relative band intensities shown in Figure 4 show much greater discrepancies between 515 and 785 nm lasers than those predicted by cross-section variation. The response

Table 2. Calculated peak area ratios for cyclohexane, relative to 801 cm^{-1} band, for different laser wavelengths.

Shift	Integration range (cm^{-1})	488 nm	514.5 nm	532 nm	632.8 nm	647 nm	785 nm ^a	1064 nm ^b (photons)	1064 nm ^c (W)
2900	2567–3068	10.70	10.484	10.343	9.547	9.437	8.40	6.480	4.898
1444	1380–1525	0.599	0.595	0.593	0.580	0.578	0.56	0.524	0.484
1267	1180–1125	0.503	0.501	0.500	0.492	0.491	0.48	0.458	0.433
1028	925–1125	0.593	0.592	0.591	0.587	0.586	0.58	0.567	0.552
801	700–900	1	1	1	1	1	1	1	1

^aThis column is the experimental average from Frost and McCreery,²⁰ other columns were calculated using equation (13). National Institute for Standards and Technology (NIST) is currently working to establish standard values for cyclohexane and other materials.

^b1064 nm laser, with photon counting detection.

^c1064 nm with detector sensitive to power (W) instead of photons per second.

function of the spectrometer is quite different for the region of 515–620 nm ($0\text{--}3300\text{ cm}^{-1}$ relative to 515 nm), compared to that for 785–1059 nm ($0\text{--}3300\text{ cm}^{-1}$ relative to 785 nm). As shown in Figure 5, the observed, uncorrected spectrum is the product of the response function and the true spectrum. The detector response at $\sim 1000\text{ nm}$ is quite weak in this case, thus attenuating the CH stretch region when observed with a 785 nm laser. The response function is the product of several instrumental variables which depend on wavelength, including detector response, mirror and grating (or beam splitter) reflectivity, lens or filter transmission, and optical alignment. Any of these can vary for instruments of different design, between instruments of the same design, or within a given instrument if a component is replaced (such as the detector). So a spectrum which is uncorrected for response function is subject to distortion relative to the true spectrum, and may vary from day to day and laboratory to laboratory. Furthermore, a properly corrected spectrum represents the actual spectrum and will remain accurate as instruments are modified and improved.

Correction for instrument response requires either an accurate knowledge of the wavelength dependence of all components in the spectrometer, or a standard source with known output. The former approach is difficult and generally impractical, so several approaches based on standard light sources or luminescent standards have been reported.^{6,20–23} Consider Figure 6, which shows the perturbation of a standard source output (Φ_L) by the response

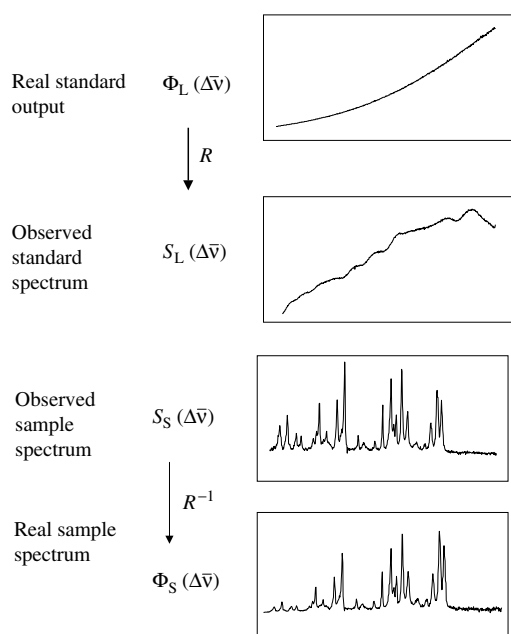


Figure 6. Overview of response function correction based on a luminescent source with known intensity vs Raman shift. S_L is the observed spectrum of a known luminescent source, and R is the spectrometer response function. (Adapted from McCreery,⁵ p. 272, with permission.)

function (R) to yield an observed spectrum (S_L). If Φ_L is known, then acquisition of S_L suffices to determine R . Once R is known, any uncorrected sample spectrum (S_S) may be divided by R to yield a corrected sample spectrum (Φ_S). Provided the standard source output is known and available in digital form, the response correction procedure may be automated through the spectrometer software. The user need only obtain a spectrum of the standard under the same conditions as those used for the sample. Alternatively, the response may be determined at the factory and stored for later use, thus relieving the user of the need to acquire and use a standard. This procedure is simpler for the user, but does not correct for drift over time or changes in alignment or optical components.

A black body radiator provides a primary standard having a known intensity vs wavelength output, and has been applied to response calibration of Raman spectrometers.²² Black body radiators are rather cumbersome, hot (obviously), and bright for use with Raman spectrometers, and it is much more common to approximate a black body with a tungsten lamp.^{6,12} The manufacturer provides a calibration of each lamp, usually based on a standard from the US NIST, which states the intensity as a function of wavelength. Since black body radiation curves depend strongly on temperature, it is critical that the power through the tungsten filament is kept constant, usually by controlling the current. An example is shown in Figure 7, for a calibrated 100 W tungsten bulb.

Although the primary issue in response function calibration is the shape of the standard emission curve, care is required in dealing with intensity units. An irradiance standard is often calibrated in units of watts cm^{-3} ,

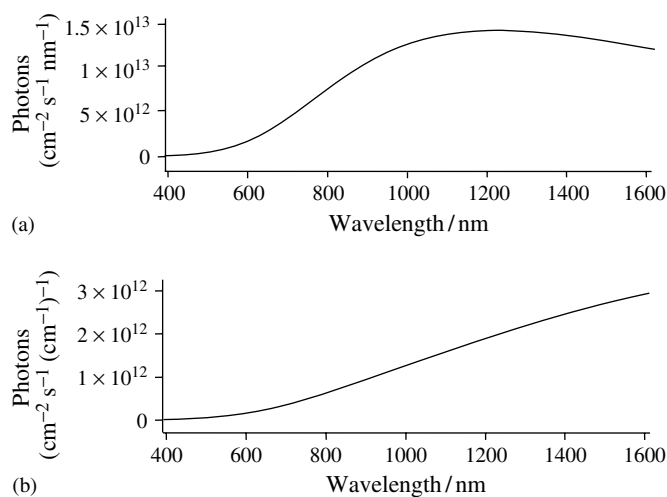


Figure 7. Output of a commercial calibrated tungsten source (Eppley Labs, Newport, RI) plotted as photons $\text{cm}^{-2}\text{ s}^{-1}$ per unit of wavelength (a) or wavenumber (b). (b) was obtained from (a) by multiplying by λ^2 . (Adapted from McCreery,⁵ p. 274, with permission.)

meaning watts cm^{-2} at a particular distance, and over a 1 cm range of wavelength. Several conversion factors which restate this intensity in more useful units are listed in equations (14)–(16).

$$I(\text{watts cm}^{-2} \text{ nm}^{-1}) = 10^{-7} I(\text{watts cm}^{-3}) \quad (14)$$

$$I(\text{photons s}^{-1} \text{ cm}^{-2} \text{ nm}^{-1}) = \left(\frac{\lambda}{hc} \right) I(\text{watts cm}^{-2} \text{ nm}^{-1}) \quad (15)$$

$$\begin{aligned} I(\text{photons s}^{-1} \text{ cm}^{-2} (\text{cm}^{-1})^{-1}) \\ = \lambda^2 I(\text{photons s}^{-1} \text{ cm}^{-2} \text{ nm}^{-1}) \end{aligned} \quad (16)$$

Equation (16) results from the fact that the wavenumber and wavelength axes are inversely related rather than proportional, and

$$d\tilde{\nu}(\text{cm}^{-1}) = \frac{d\lambda(\text{nm})}{\lambda^2} \times 10^{17} \quad (17)$$

Figure 7 shows intensity curves for two sets of units, demonstrating that both magnitude and shape depend on how the intensity is stated. For all cases noted in equations (14)–(17), λ refers to the absolute wavelength and $\tilde{\nu}$ the absolute wavenumber.

A more recent alternative to a black body or tungsten source is a luminescent standard which emits a known intensity vs wavelength curve when illuminated by the laser.^{20,21,23} The standard can be a solid such as rare-earth doped glass, or a solution of a fluorescent molecule. The standard is positioned as if it were an ordinary sample, and illuminated with the laser as usual. The illuminated standard emits an intensity vs wavelength curve similar to those shown in Figure 8, which is monitored by the spectrometer. The standard's output is calibrated against a black body radiator by its manufacturer, resulting in a

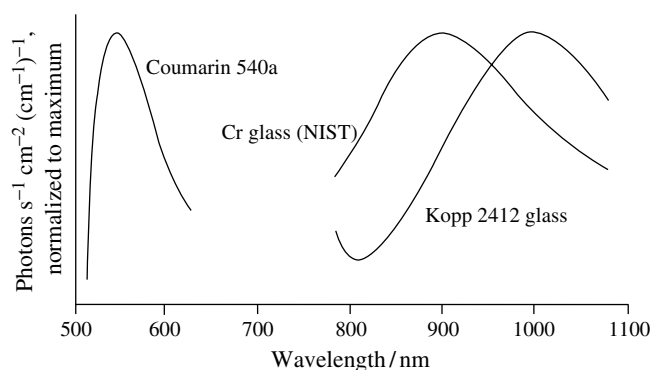


Figure 8. Output of three luminescent standards when illuminated by 514.5 nm (Coumarin) or 785 nm (NIST and Kopp) lasers. Curves were calculated from polynomials accompanying each standard, and normalized to maximum intensity. Note that the ordinate states intensity per unit of Raman shift (in cm^{-1}), while the abscissa is in nanometers to permit coverage of a wide range.

polynomial which states the intensity of emission vs Raman shift relative to a specified laser, such as that shown in Figure 6.

A luminescent intensity standard has several advantages over a tungsten bulb for calibrating the instrument response function. First, the standard is treated like “just another sample” and does not require additional apparatus. Second, the standard duplicates the Raman sampling geometry and sample position, ensuring that the standard emission follows the same light path as the Raman light to be calibrated. Third, the luminescent output is proportioned to laser power, permitting an automatic correction for day-to-day variation in laser power. Fourth, the luminescent output curve is not dependent on a regulated power supply, so drift or distortions in the emission curve shape are less likely. Fifth, the standard may be placed inside a sample container or behind a window, thus correcting for response function changes caused by the sampling mode. In practice, these advantages simplify the calibration procedure so that the response function may be rapidly determined any time the instrument settings or components are changed, thus making the response function correction fast, inexpensive and routine.

Accompanying these advantages are some constraints on the use of luminescent standards in place of a tungsten bulb. Each luminescent standard must be calibrated for a particular laser wavelength, while a tungsten source may be used throughout the visible and NIR regions. Although a luminescent standard reproduces sampling geometry more accurately than a tungsten bulb, the match is not perfect. Luminescent standards usually absorb the laser light, resulting in a different penetration depth from that in the Raman sample. Finally, luminescent standards must be verified to be stable for the laser powers in use, and to be optically homogeneous.

Once implemented, a response function correction derived from either a tungsten bulb or luminescent sample corrects for a variety of intensity distortions caused by the spectrometer. For either CCD- or FT-Raman spectrometers, the procedure corrects for the variation of detector response and filter transmission with wavelength, which are two major sources of intensity distortion. Figure 5 shows a common distortion caused by interference effects in the laser rejection filter, which appear as baseline modulation in the region of $300\text{--}800\text{ cm}^{-1}$. Such artifacts are accurately corrected with a response function calibration. In FT-Raman spectrometers, the procedure corrects for variation in beamsplitter transmission and interferometer mirror reflectivity with wavelength.

Dispersive Raman spectrometers with CCD detection can produce additional intensity artifacts which are corrected by a response function calibration. First, fabrication of

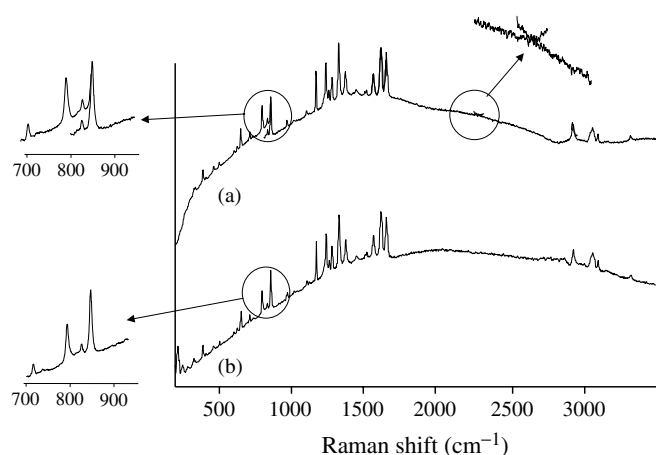


Figure 9. Correction of discontinuities which occur when dispersive/CCD segments are combined. (a) Spectrum is uncorrected, and consists of five CCD accumulations, with discontinuities apparent near 810 and 2300 cm^{-1} . Discontinuities at “splices” are removed in (b), using an instrument response correction based on a luminescent standard. (Adapted from McCreery,⁵ p. 210, with permission.)

the CCD may lead to variation in pixel sensitivity which repeats across the CCD, often in groups of four. This “fixed pattern variation” appears to be noise, and can be a particular problem for small Raman peaks on top of high background. Second, CCD spectra are often “spliced” from several exposures of different regions of the spectrum. Discontinuities occur at splices because the optical paths for wavelengths near the splice are different for the two segments being spliced. As shown in Figure 9, such artefacts are accurately corrected by a response correction. Third, gain variations caused by “hot” or “weak” pixels may occur from defects in the CCD substrate. Provided a particular pixel is at least partially photoresponsive and does not saturate, a response correction can correct aberrations in pixel sensitivity.

Speaking more generally about either FT or CCD Raman spectrometers, the success of a response correction depends on the accuracy of the standard emission curve (Figure 7a and Figure 8) and the degree to which the sample acquisition parameters duplicate those of the standard. Ideally, the emission of the standard occurs over an area and depth which match those from which Raman scattering occurs. Provided the spectrometer observes an accurately known emission from a standard, a response correction accurately corrects for a wide variety of spectrometer artifacts. In fact, a luminescent standard is functionally analogous to the reference channel of a double beam UV–vis spectrometer, in that it provides a known reference intensity which calibrates the spectrometer optics, detector, and any data acquisition properties. In principle, at least, a luminescent standard could also correct for solvent absorption, such as might

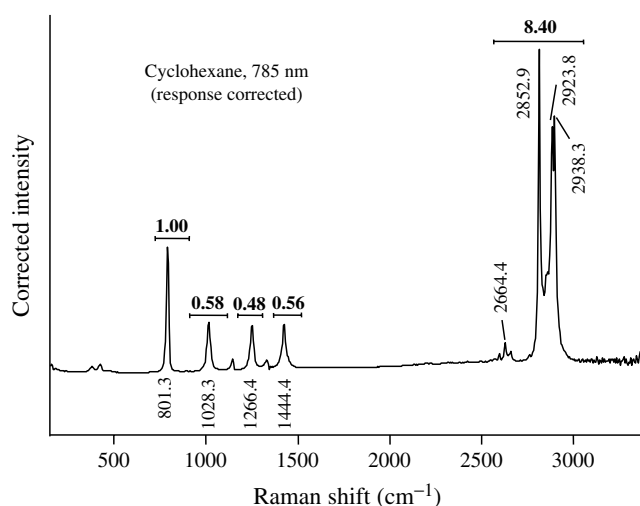


Figure 10. Response corrected spectrum of cyclohexane, 180° backscattered geometry, parallel and perpendicular polarizations monitored, 785 nm excitation. Horizontal bars indicate integration limits and relative peak areas, and are included in Table 2. Relative peak area ratios are currently being verified by NIST, in order to establish standard values. Smaller numbers are American Society for Testing and Materials (ASTM) standard E 1840 Raman shifts of indicated bands. (Adapted from McCreery,⁵ p. 280, with permission.)

occur from overtones of vibrational modes (in the NIR), or colored samples (in the visible). The standard would have to be dissolved in the solvent of interest, and the effective path lengths would need to match, so correction for solvent absorption would require significant care.

Once a response correction procedure is in place, its accuracy should be verified with standards having known relative Raman intensities. For example, the corrected spectrum of a common solvent could be normalized to the band area of a given Raman feature, and the relative peak areas of the remaining bands could be tabulated. Figure 10 shows such a spectrum for liquid cyclohexane and a 785 nm laser. Predicted ratios for cyclohexane, based on experimental results at 785 nm, were listed in Table 2, normalized to the 801 cm^{-1} band area at each wavelength. At the time of this writing, there are no established relative intensity standards sanctioned by NIST or the ASTM. The two organizations are currently testing luminescent standards, and determining accurate peak area ratios for common materials such as cyclohexane, benzonitrile, naphthalene, etc. The objective is to provide corrected spectra for the ASTM Raman shift standards, to permit instrument users and manufacturer to verify the accuracy of whatever response correction they employ. Table 3 lists relative peak areas for several solvents and air, for 785 and 514.5 nm excitation. As response correction becomes more common, the ratios listed in Table 3 will be refined, and it is likely that standards with certified area ratios will become available.

Table 3. Response corrected relative peak areas.^a

Sample (all pure liquids)	514.5 nm, literature	514.5 nm, corrected with Coumarin 540a	785 nm, literature	785 nm, corrected with Kopp 2412 glass
CH ₂ Cl ₂ 288 cm ⁻¹ (225–360 cm ⁻¹) ^b			0.58 ^c	0.48 ± 0.03 (<i>N</i> = 16) ^d
702 cm ⁻¹ (600–850)	1.00	1.00	1.00	
2988 cm ⁻¹ (2900–3150)	0.74 ^c	0.83 ± 0.12 (<i>N</i> = 18) ^d	0.58 ^c	0.66 ± 0.06 (<i>N</i> = 17)
CHCl ₃ 260 cm ⁻¹ (205–470) ^b			1.12 ^c , 1.02 ^e	1.00 ± 0.03 (<i>N</i> = 11)
364 (205–470) ^b			1.13 ^c , 1.03 ^e	0.97 ± 0.03 (<i>N</i> = 11)
666 (550–900)			1.00	
758 (550–900)			0.56 ^c , 0.62 ^e	0.50 ± 0.07 (<i>N</i> = 11)
3021 (2920–3120)			0.42 ^c , 0.48 ^e	0.47 ± 0.06 (<i>N</i> = 11)
Benzene 992 (900–1100)	1.00	1.00	1.00	
3060 (2960–3160)	0.99 ^c , 1.17 ^e , 1.48 ^h	1.05 ± 0.16 (<i>N</i> = 12)	0.80 ^c , 0.92 ^e , 1.26 ^f	0.87 ± 0.05 (<i>N</i> = 14)
Acetonitrile 919 cm ⁻¹ (825–1025)		1.00	1.00	
2254 (2150–2400)	4.0 ^f , 3.3 ^b	3.86 (<i>N</i> = 2)	3.19 ^g , 2.88 ^c	3.31 (<i>N</i> = 2)
2943 (2800–3150)	7.23 ^c	9.71 (<i>N</i> = 2)	5.83 ^c	7.79 (<i>N</i> = 2)
Cyclohexane 801 (700–900)		1.00	1.00	
1028 (925–1125)			0.58 ^c	0.63 ± 0.03 (<i>N</i> = 11)
1267 (1180–1315)			0.49 ^c	0.52 ± 0.02 (<i>N</i> = 11)
1444 (1380–1525)			0.64 ^c	0.65 ± 0.04 (<i>N</i> = 11)
All CH (2587–3068)			6.50 ^c	7.38 ± 0.76 (<i>N</i> = 11)
Air 1555 (O ₂) (1450–1650)	1.00			
2331 (N ₂) (2225–2425)	3.26 ⁱ	3.22 ± 0.04 (<i>N</i> = 3) ^j		

^a Adapted from Frost and McCreery,²⁰ including all observed results from two spectrometers. NIST is currently verifying these results and establishing standards. For cyclohexane, Table 2 includes more current values from three independent laboratories.

^b Integration range for peak area. The CHCl₃ 260 and 364 cm⁻¹ bands were integrated as two bands within the 205–470 cm⁻¹ range.

^c Calculated from Nestor and Lippincott,²⁴ using equation (13).

^d Stated as mean ± standard deviation. *N* = number of spectra analyzed.

^e Calculated from Schrötter and Klöckner,⁹ using equation (13), then converted to liquid values using liquid/gas ratios in Schrötter and Klöckner,⁹ Table 4.6.

^f Calculated from Schomacker *et al.*¹³ by adjusting reported 514.5 nm cross-sections by $\bar{\nu}_O(\bar{\nu}_O - \bar{\nu}_j)^3$.

^g Calculated using “A” term parameters and equation (11) of Dudik *et al.*¹²

^h Reported in Schomacker, *et al.*¹³

ⁱ Calculated from Schrötter and Klöckner,⁹ for 21% O₂, 78% N₂.

^j For Chromex 250 spectrograph with custom 180° collection optics.

Table 4. Absolute Raman cross-sections.^a

Sample	Laser λ (nm)	β^b ($\text{cm}^2 \text{sr}^{-1}$ molecule ⁻¹) $\times 10^{30}$	β^c ($\text{cm}^6 \text{sr}^{-1}$ molecule) $\times 10^{48}$	Reference ^c
Benzene liquid, 992 cm^{-1}	647	10.6		25
	514.5	30.6		13
	514.5	28.6		26
	514.5	27.0	235	9
	488	36.5		13
	441.6	44.6		13
	407	64		15
	351	160		15
	337	392	580	9
	325	440		13
	351–694			259 \pm 66 ^d
1% benzene in CH_3CN	514.5	19.2		12
	220	15.2		12
Benzene liquid, 3060 cm^{-1}	514.5	45.3		13
	488.0	57.1		13
	441.6	68.3		13
	325.0	477		13
Benzene gas, 992 cm^{-1}	514.5	7.0	61	9
Cyclohexane liquid, 802 cm^{-1}	647	2.1		15
	514.5	5.2		15
	488	9.06		24
	407	17.6		15
Cyclohexane liquid, 1028 cm^{-1}	488	5.37		24
Cyclohexane liquid, 1267 cm^{-1}	488	4.61		24
Cyclohexane liquid, 1444 cm^{-1}	488	6.17		24
Cyclohexane liquid, all C–H	647	12.7		15
	514.5	43		15
	488	75.2		24
	407	127		15
N_2 gas, 2331 cm^{-1}	514.5	0.43	5.01	9
	488.0	0.54	5.06	9
	457.9	0.74	5.1	9
	351.1	2.43	5.2	9
O_2 gas, 1555 cm^{-1}	514.5	0.58	5.0	9
CH_3Cl gas, 725 cm^{-1}	514.5	1.73	14.1 ^a	9
CH_2Cl_2 gas, 2997 cm^{-1}	546.1	1.71	23.4 ^a	9
CH_2Cl_2 gas, 713 cm^{-1}	546.1	2.29	18.6 ^a	9
CH_3CN , 918 cm^{-1}	514.5	1.00		12
	220	41.6		12
CH_3CN , 2249 cm^{-1}	514.5	8.22		12
	220	399		12
CHCl_3 gas	3032 cm^{-1}	0.59	8.2 ^e	9
	1221 cm^{-1}	0.19	1.7 ^e	9
	758 cm^{-1}	1.1	8.7 ^e	9
	667 cm^{-1}	1.7	13.8 ^e	9
	364 cm^{-1}	1.7	12.6 ^e	9
	261 cm^{-1}	1.8	13.3 ^e	9
CCl_4 gas	459 cm^{-1}	4.7	36.4	9
	221 cm^{-1}	2.4	17.9	9

Table 4. (continued)

Sample	Laser λ (nm)	β^b ($\text{cm}^2 \text{sr}^{-1}$ molecule $^{-1}$) $\times 10^{30}$	β^c ($\text{cm}^6 \text{sr}^{-1}$ molecule) $\times 10^{48}$	Reference ^e
ClO_4^- in water, 932 cm^{-1}	514.5	12.7		12
SO_4^- in water, 981 cm^{-1}	514.5	9.9		12
NO_3^- in water, 1045 cm^{-1}	514.5	10.9		12
ClO_4^- in water, 932 cm^{-1}	220	772		12
SO_4^- in water, 981 cm^{-1}	220	601		12
NO_3^- in water, 1045 cm^{-1}	220	799		12
Cacodylate, 608 and 628 cm^{-1}	647	3.2		15
	514.5	14.3		15
	407	39		15

^aBoth parallel and perpendicular polarizations observed.

^bBased on classical $\bar{\nu}^4$ dependence. May be converted to dependence on equation (2) by multiplying by $\bar{\nu}_0/(\bar{\nu}_0 - \bar{\nu}_j)$.

^cSchrötter and Klöckner⁹ give many more gas phase cross-sections. β^c values listed here are averaged when Schrötter and Klöckner list several values.

^dMean and standard deviation of 19 values from Petty *et al.*²⁵

^e β^c based on 546.1 nm excitation, β calculated for 514.5 using $\bar{\nu}^4$ dependence.

6 DETERMINATION OF ABSOLUTE RAMAN CROSS-SECTIONS

Once a Raman spectrum is corrected for instrument response, the area under a given band is proportional to the cross-section β . β is a “differential” cross-section because the designation refers to photons scattered over some increment of solid angle (hence the common designation $d\sigma/d\Omega$). β varies with observation angle, particularly for polarized bands or oriented samples such as crystals or surfaces. The integrated Raman cross-section, σ , is the integral of β over all solid angles, and represents the total scattering into a spherical collector. Since nearly all Raman spectrometers sample a small range of solid angle, the measured intensity depends on the value of β which applies to the angle between the laser and the collection axis. Since Raman scattering is partially or fully polarized, the cross-section also depends on any polarization sensitive components in the spectrometer or optical geometry. The integrated cross-section for an isotropic sample does not depend upon observation geometry or polarization, but it is very rarely used because total Raman scattering is rarely determined in practice. There is no consensus about a standard geometry, although 180° backscattering and 90° illumination are quite common. When comparing cross-sections, the user should be aware of the collection geometry and polarization.

Although the number of absolute Raman cross-sections available in the literature is fairly small, they are quite informative. A corrected spectrum showing relative peak areas (and therefore relative cross-sections) may be sufficient for sample identification, but the absolute cross-section provides an indication of which compounds are “strong” or “weak” scatterers. The sensitivity of chemical analysis

based on Raman scattering may be assessed directly from the absolute cross-section, if known. The variation of cross-section with laser wavelength is of fundamental importance to investigations of resonance Raman scattering, and generally requires both response correction and absolute cross-section determination.^{11,12}

A practical procedure for determining absolute cross-sections is comparison of a response corrected spectrum to that of a standard with known cross-section. For example, the 992 cm^{-1} band of liquid benzene has a generally accepted value of $2.86 \times 10^{-29} \text{cm}^2 \text{molecule}^{-1} \text{sr}^{-1}$ for 514.5 nm excitation. The peak area of a Raman feature in a response corrected spectrum may be compared to a spectrum of benzene acquired and corrected in the same manner. The ratio of the peak area of the feature of interest to that of the 992 cm^{-1} band of benzene equals the ratio of absolute cross-sections. Provided the sample absorbs neither the laser nor the Raman scattered light, and the other optical properties of the standard and sample are identical, this procedure yields accurate results. In many cases, it is possible to dissolve a standard and sample in the same solvent, so acquisition conditions are identical. The cross-section of the standard may change upon dilution due to local field effects, so the standard cross-section should be obtained in conditions which duplicate those of the sample as much as possible. The difficulty of determining absolute cross-sections, along with their dependence on scattering geometry, has resulted in some disparity among literature values for proposed standards. Several cross-sections are listed in Table 4, for various laser wavelengths.

If the user’s objective involves quantitative comparison of Raman scattering intensity, but does not require determination of the cross-section, a significantly simpler procedure

has been reported.²⁵ A Raman band of a standard is chosen as a reference, and Raman bands of samples are compared for the same experimental conditions. Provided the spectra are reproducible and corrected for instrument response, the band areas of the sample may be quantitatively compared to the standard. A Raman intensity scale based on this approach has been proposed.²⁵

ABBREVIATIONS AND ACRONYMS

ASTM	American Society for Testing and Materials
NIST	National Institute for Standards and Technology
RSD	Relative Standard Deviation
UV-vis	Ultraviolet-Visible

REFERENCES

1. J.G. Graselli and B. Bulkin, 'Analytical Raman Spectroscopy', Wiley & Sons, New York (1991).
2. R.L. McCreery, 'CCD Array Detectors for Multichannel Raman Spectroscopy', in "Charge Transfer Devices in Spectroscopy", eds J. Sweedler, K. Ratzlaff and M. Denton, VCH, New York, 227-279 (1994).
3. M.J. Pelletier, 'Analytical Applications of Raman Spectroscopy,' Blackwell Science Ltd, London (1999).
4. D.B. Chase and J.-F. Rabolt, 'Fourier Transform Raman Spectroscopy: From Concept to Experiment', Academic Press, New York (1994).
5. R.L. McCreery, 'Raman Spectroscopy for Chemical Analysis', Wiley Chemical Analysis Series, ed. J. Winefordner, Wiley & Sons, New York (2000).
6. M. Fryling, C.J. Frank and R.L. McCreery, *Appl. Spectrosc.*, **47**, 1965 (1993).
7. R.L. McCreery, 'Raman Spectroscopy for Chemical Analysis', Wiley Chemical Analysis Series, ed. J. Winefordner, Wiley & Sons, New York, Chapter 2 (2000).
8. A. Weber (ed.), 'Raman Spectroscopy of Gases and Liquids', in "Topics in Current Physics", Springer-Verlag, New York, Vol. 11 (1979).
9. W. Schrötter and H.W. Klöckner, 'Raman Scattering Cross-Sections in Gases and Liquids', in "Topics in Current Physics", Springer-Verlag, New York, Vol. 11, Chapter 4 (1979).
10. A.C. Albrecht and M.C. Huntley, *J. Chem. Phys.*, **55**, 4438(71).
11. S.A. Asher and C.R. Johnson, *J. Phys. Chem.*, **89**, 1375 (1985).
12. J.M. Dudik, C.R. Johnson and S.A. Asher, *Chem. Phys.*, **82**, 1732 (1985).
13. K.T. Schomacker, J.K. Delaney and P.M. Champion, *J. Chem. Phys.*, **85**, 4240 (1986).
14. B. Li and A.B. Myers, *J. Phys. Chem.*, **94**, 4051 (1990).
15. M.O. Trulson and R.A. Mathies, *J. Chem. Phys.*, **84**, 2068 (1986).
16. M. Ludwig and S.A. Asher, *Appl. Spectrosc.*, **42**, 1458 (1988).
17. R.L. McCreery, 'Raman Spectroscopy for Chemical Analysis', Wiley Chemical Analysis Series, ed. J. Winefordner, Wiley & Sons, New York, Chapter 3 (2000).
18. R.L. McCreery, 'Raman Spectroscopy for Chemical Analysis', Wiley Chemical Analysis Series, ed. J. Winefordner, Wiley & Sons, New York, 103-106, 295-300 (2000).
19. Yan Wang Alsmeyer and R.L. McCreery, *Anal. Chem.*, **63**, 1289 (1991).
20. K.J. Frost and R.L. McCreery, *Appl. Spectrosc.*, **52**, 1614 (1998).
21. K.G. Ray and R.L. McCreery, *Appl. Spectrosc.*, **51**, 108 (1997).
22. C.J. Petty, G.M. Warnes, P.J. Hendra and M. Judkins, *Spectrochim. Acta*, **47A**, 1179 (1991).
23. H. Hamaguchi, *Appl. Spectrosc. Rev.*, **24**, 137 (1988).
24. J.R. Nestor and E.R. Lippincott, *J. Raman Spectrosc.*, **1**, 305 (1973).
25. C.J. Petty, P.J. Hendra and T. Jawhari, *Spectrochim. Acta*, **47A**, 1189 (1991).